Ann. Geophysicae 16, 711–720 (1998) © EGS – Springer-Verlag 1998

Annales Geophysicae

Non-trough *fo*F2 enhancements at near-equatorial dip latitudes

E. Sambou[1], **P. M. Vila**[2], **A. T. Kobea**[3]

[1] Département de Physique, Université C. Anta Diop, Dakar-Fann, Senegal
[2] Centre d'Étude des Environnements Terrestres et Planétaires (CETP), 4 Avenue de Neptune, F-94107, Saint-Maur-des-Fossés, France
[3] Département de Physique de l'Atmosphère, Université de Cocody, 22 BP582, Abidjan 22, Côte d'Ivoire

Received: 9 December 1996 / Revised: 26 November 1997 / Accepted: 2 December 1997

Abstract. Fine resolution series from three equatorial ionosondes of the IEEY network in West Africa have revealed small-scale daytime peak F2 structures, superposed on the slowly varying minimum or "trough" distribution in the ±5° magnetic latitude zone. We report this new morphology, concentrating on *fo*F2 enhancements of two types: near-equatorial crests (which travel either northwards or southwards) and magnetic field-aligned domes, whose onsets last only tens of minutes. Both types are observed to start at mid-morning or early afternoon hours. We relate their occurrence with the available variations of $\mathbf{Vz} = \mathbf{E} \times \mathbf{B}$ upward drift which feeds the equatorial plasma fountain. We suggest the *fo*F2 enhancements to be triggered by brief slow-downs of the $\mathbf{Vz}$ velocity near F2 peak altitude in our West African sector. Their short latitude extent differentiates them from the larger-scale tropical crest system. Further analysis of these features should lead to weather-like models of the low latitude ionosphere variations, where unstable local coupling between processes seems to be the trigger.

Key words. Ionosphere (Equatorial ionosphere · Ionosphere-atmosphere interaction · Plasma temperature and density)

1 Introduction

The F2 layer plasma density is everywhere controlled by a balance between EUV production, photochemical loss and the divergence of plasma flux. Gravity and pressure gradients cause plasma to diffuse parallel to the magnetic field lines while perpendicular motion depends mostly on $\mathbf{E} \times \mathbf{B}$ vertical drift. At equatorial magnetic latitudes the divergence term is quite characteristic: its magnetic symmetry is nearly perfect because magnetic tubes have long horizontal dimensions. During most of daytime the $\mathbf{Vz} = \mathbf{E} \times \mathbf{B}$ drift is upwards as the driving $\mathbf{E}$y zonal field is directed eastward. Under this upward drift associated with the E layer electrojet regime, a fountain mechanism removes the plasma on both north and south sides of the equatorial F layer area, generating a "trough" or latitude minimum of peak F2 density.

This minimum is classically modulated by the diurnal variation of the driving electric field, and the whole equatorial area exhibits a "noon bite-out" relative minimum. Following the results of the International Geophysical Years 1958-1959 the F2 peak ionization structure showing these two "anomalous" aspects (Appleton 1960) was named the Appleton anomaly, or more recently "Equatorial Ionization Anomaly, EIA". Although inappropriate this latter denomination has remained; it popularizes the basic concept of a stationary fountain mechanism leading to dense "crests" on both tropics with a central trough over the equatorial electrojet zone. Indeed this mesoscale structure was repeatedly validated for magnetically quiet periods between about 1000 and 2200 LT, suggesting a steady-state plasma fountain regime. Following substorm electric field reversals at the magnetic equator and also large counter-electrojet events, this structure presents local distortions. After strong magnetic storms it can be replaced either by a single dome, or by a wide plateau covering the whole intertropical F2 space (Vila, 1971a, b). Until very recently the quiet-time density structure of two tropical crests has been validated by many observations, especially at solar flux maximum (Rastogi, 1959; Lyon and Thomas, 1963) and minimum periods (Vila, 1971a, b; Rastogi, 1959). Corresponding measurements of vertical drift have been made with the I.S. radar at Jicamarca (reviewed by Fejer and de Paula, 1995) and by various in situ probes on DE-2 (Coley and Heelis, 1989), and AE-E satellites. They agreed very well with the time-dependent models of Hanson and Moffett

Correspondence to: P. M. Vila

(1966) and Abur-Robb and Windle (1969). There remained a lack of detailed information on the shape and development of the anomaly for a narrow latitudinal sector. In the present study we attempt to describe the form and the development of the electron density distribution in the "trough".

We discuss the recent IEEY (November 1992 to November 1994) data from three ionosondes at Dakar (Senegal), dip latitude 5°N; Ouagadougou (Burkina-Faso) dip latitude 1.5°N and Korhogo (Ivory-Coast) dip latitude 2°S, located inside the trough zone. By contrast, they show intense short-period distortions in *f*oF2 peak density which did not appear in 1966, and which passed unnoticed in other published work. These enhancement types which occur exactly at the dip equator are respectively moving trans-equatorial crests and quiet-day domes, and we will restrict our work to their formation processes. In the second section we describe the equatorial crest and dome morphology, and present their main LT and seasonal fluctuations. In a third section we qualitatively speculate about the probable slow-down plasma motion processes at the origin of crests and domes at the magnetic equator. We briefly mention another possible mechanism for mid-morning enhancements due to persistent photo-electron heating, compatible with crests and domes without change of the vertical F2 peak density scale height.

2 Morphology

2.1 The classical equatorial trough model

During magnetically quiet day time at the magnetic equator, the polarization electric field of E layer dynamo origin is pointing eastwards. It is mapped into the F layer by the magnetic lines of force. In the F region the plasma transport across the magnetic field is controlled by the $\mathbf{E} \times \mathbf{B}$ drift. Charge particles are lifted by $\mathbf{E} \times \mathbf{B} = \mathbf{Vz}$ drift velocity (which generally reverts downward during the night). Quiet day-time drift carries the plasma at altitudes up to 700 km above the F2 peak (at 300 to 450 km altitudes). The plasma is then displaced by ambipolar diffusion along magnetic lines of force under gravity and plasma pressure gradients (Martyn, 1947; Duncan, 1960; Anderson, 1973, 1981). This is the fountain mechanism first physically modelled by Hanson and Moffett (1966): the coupled orthogonal rise and field-aligned motions accumulate plasma towards F2 peak levels at tropical magnetic latitudes of about 15° north and south.

The latitude profiles of F2 peak density (related to *f*oF2 measured critical frequency by the relation $N = 1.24 \cdot 10^4 \cdot (f\text{oF2})^2$ remain smooth at daytime hours with a minimum centred at the dip equator, in the general appearance of a "trough". In LT this trough is modulated along a "noon bite-out" shape due to the stronger upward-drift velocity at midday hours. This structure has been studied by many workers using ionosonde data (Walker, 1981).

Until our IEEY programme was developed the quiet day-time *f*oF2 equatorial structure was believed to vary only slightly from 0900 to 1800 LT. Only smooth morning and/or evening peaks were observed, with magnetic and seasonal dependences.

2.2 The new foF2 equatorial morphology

Presentation of the data. On Fig. 1a we show a trough-type plot of the *f*oF2 (UT) variations at our three stations together, which materialize fixed-latitude chan-

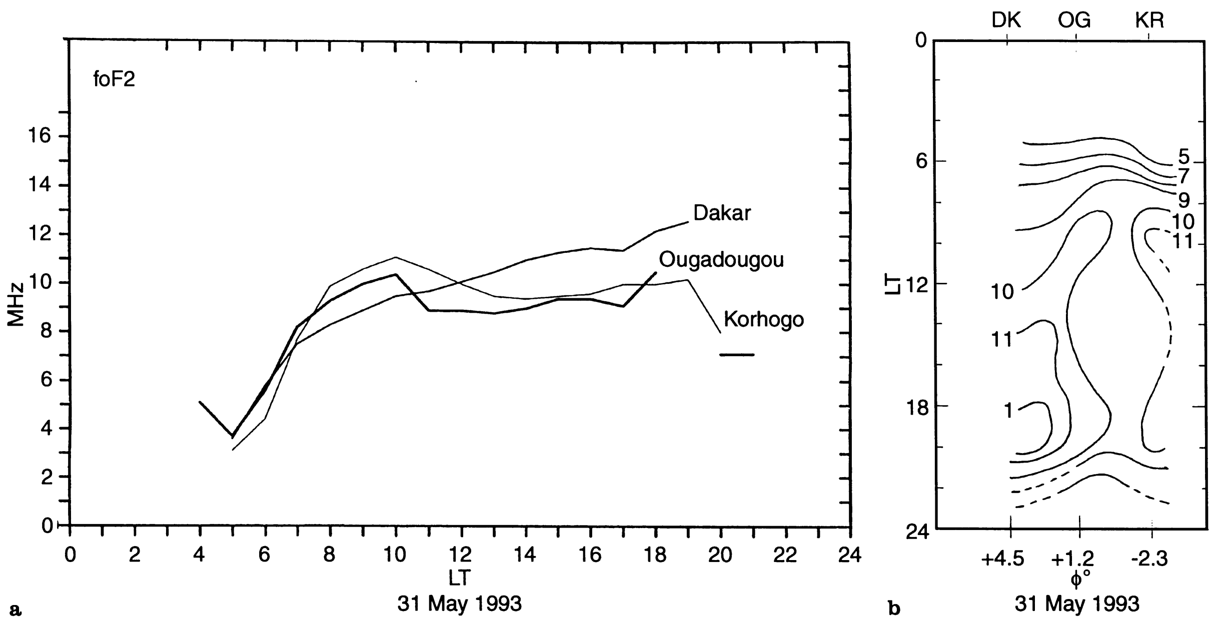

Fig. 1. Peak F2 equatorial "trough" variations, 31 May 1993: **a** *f*oF2(UT) curves for the three stations: Dakar, Ouagadougou, Korhogo. **b** corresponding *f*oF2 (magnetic latitude, LT) contour chart. X axis: latitude (North to left); y axis: LT increasing down. The *vertical bar* marks the dip equator

ges, but do not display local time variation. The dynamics is much clearer if the variations can be ordered in a common magnetic meridian; in our case this is obtained by using a common LT referential. We have drawn the same *f*oF2 variations, interpolating contours in a corrected LT and latitude referential to replace the variations in a near-common magnetic meridian on Fig. 1b. The latitude horizontal axis points to north on the left while the vertical axes LT increases downwards, and the magnetic equator is marked by a vertical line. Across the longitude span of 16° of our stations the dip equator latitude is almost stationary. This allows us to reduce the data to an average meridian, the very low dip latitude keeping the west magnetic declination effect undetectable (for simplicity we shift the time scales of Dakar and Korhogo variations onto those at Ouagadougou, bringing the network data into a common UT approximate reference). With this LT alignment the distribution patterns become remarkably consistent. On Fig. 1b the *f*oF2 contours show the usual "anomaly" trough structure dominant from 0830 to 1930 LT.

Figure 2 is a comparison of similar presentation for *f*oF2 across the entire intertropical latitude domain in West Africa (1966) which shows a smooth and uniform trough (Vila, 1971a). We use thin lines to show the extreme 5° dip latitude span of our IEEY network acquisition zone. Figures 1b and 2 give similar contours inside these limits. Contrary to all previous results, in 1993–1994 continuous troughs exist only during the March to November period, and their average occurrence is less than 50%.

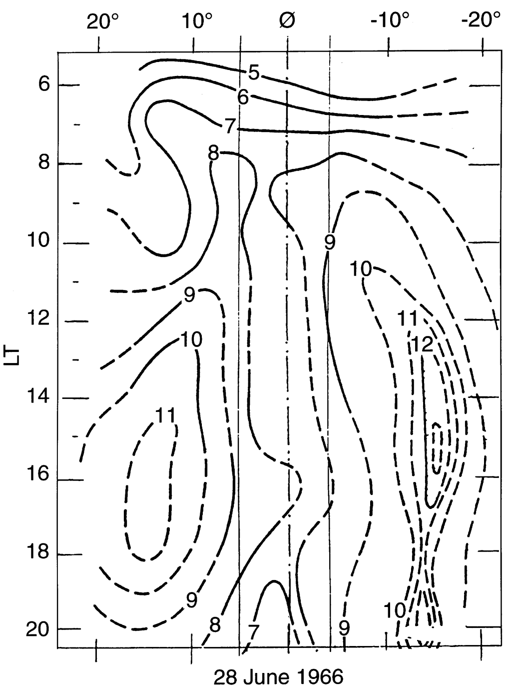

Fig. 2. Classical *f*oF2 contours at low latitudes showing intertropical crest evolution over the whole ±20° magnetic latitude for a quiet day 1966, central African network

Typical F2 peak enhancements are shown on Fig. 4b for an "equatorial crest" type c and on Fig. 6b for a "dome" structure. In both cases the density is enhanced relative to the adjacent trough value by a factor of 2.

2.3 Description of the abnormal equatorial foF2 distributions

We had to create new names for equatorial plasma density features when we realized that they no longer fitted the earlier mid-morning origins and afternoon ends of the main intertropical crest structure.

Figure 3 summarizes the six morphological types. The top panels describe the various trough evolutions and show:

b_s: for sinuous trough change in LT
a: for the "normal" trough variation
b_g: for giant troughs

The bottom panels illustrate the most frequent distortions:

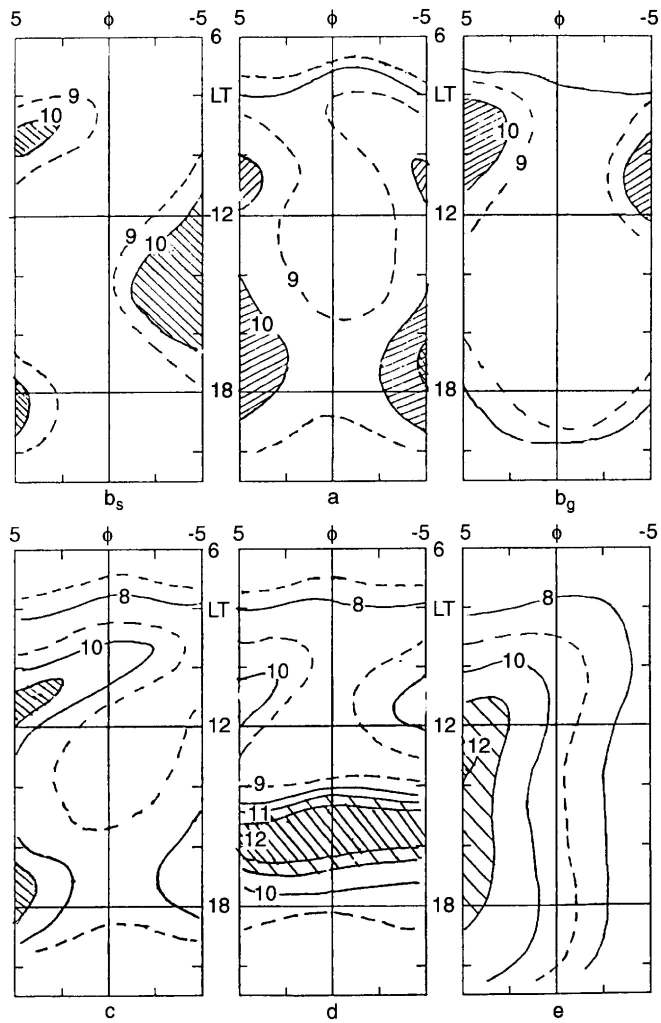

Fig. 3. Schematic morphologies – *upper row*: three trough-like types; *bottom row*: frame *c* for morning northern crest, frame *d* for morning trough and afternoon dometype, frame *e* for magnetic field-perpendicular gradient (November to February)

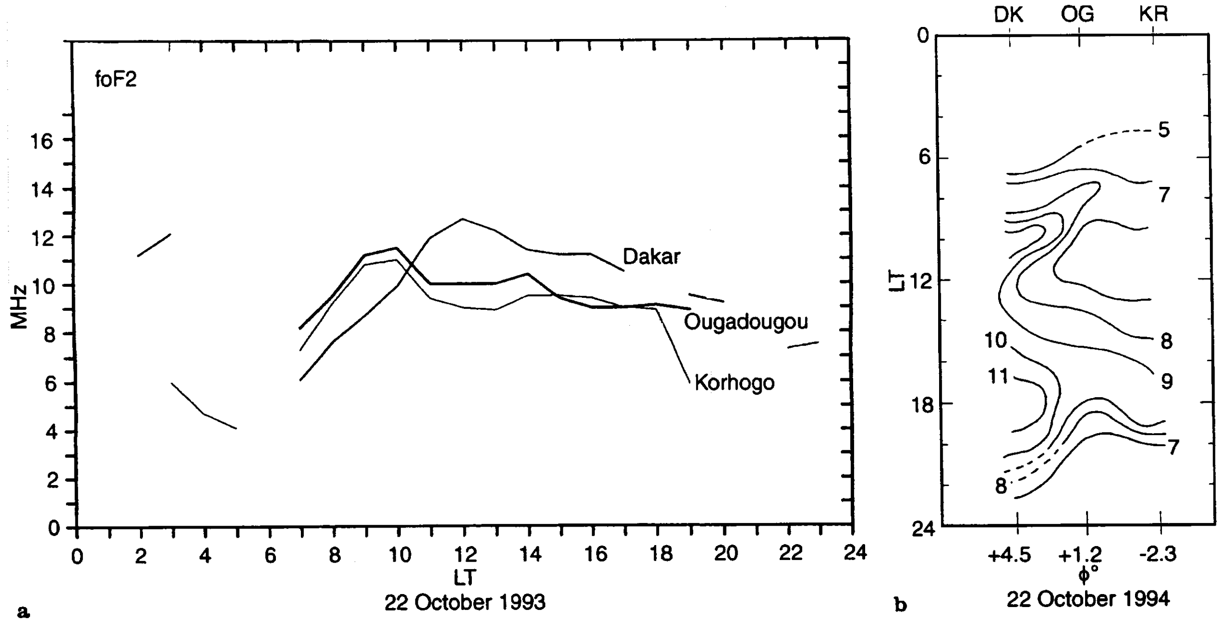

Fig. 4. Example of crest-type event for 22 October 1993, morning and afternoon northern crest events. **a** *f*oF2(UT) curves, **b** corresponding *f*oF2 contour chart

c: for equatorial crest events
d: for quiet-time domes
e: for nearly uniform northward gradient, which dominates our contours during local winter from November to February.

2.4 Observed typical contours

In this study we shall concentrate principally on crest and dome events such as "*C*" *Crests* (example Fig. 4).

These generally cross the magnetic equator especially the morning crests. They differ from the background *f*oF2 variation in their short life times and their recurrence. They occur distinctively from March to October with more than 50% abundance (irrespective of magnetic activity except for strong post-storm periods). Figure 5 shows combined monthly percentages of crest abundance in 1993 for morning and afternoon types, i.e. for local times centred on 1000 and 1430. The number of events for each type are marked at the top of the corresponding bars. Diurnal progression of crests, if extrapolated to higher latitudes between 11:00 and 16:00 LT, would never bring their maximum distance farther than 9° dip latitude. Their width on the LT-latitude pattern (less than 2 h and less than 3°) is too limited to correspond to the slow phases of the fountain motions as documented in intertropical morphologies. Therefore equatorial crests are a distinct structure from the classical tropical ones.

"*d*" *domes* (Fig. 6a, b; here the morning dome arises between 0830 and 1030 LT). The north-south alignment and the rapid formation phases (less than one hour) are quite incompatible with the slow evolution of the Appleton anomaly.

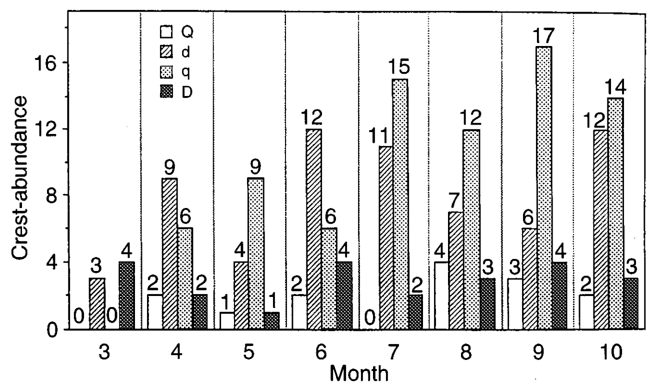

Fig. 5. Histograms of monthly crest abundances distributed into four magnetic activity ranges according to the relevant sums of 8 three-hourly am indices (between noon on the previous day and noon on the day considered: Q (very quiet): $\sum a_m < 10; q$ (quiet): $10 \leq \sum a_m < 20 d$ (moderately active): $20 \leq \sum a_m \leq 30; D$ (disturbed): $\sum a_m > 30$ (sampling interval Feb.–Nov. 1993).

The general appearance is of a single magnetic field-aligned wave with an abrupt onset. Domes occur at the same local times as the crest types. Afternoon enhancements on the southern side of our zone sometimes prolong these events; they probably result from the wind asymmetric drag of an early diurnal reversal.

The geographic scales involved in crest and dome formation appear comparable to those of evening ESF triggers. However our events differ by their enhancement character (instead of ESF depletions), their regular onset times and their first appearance at peak F2 level. Neither crest nor dome occurrence depend clearly on magnetic activity levels. Magnetic storms generate much larger domes which invade the whole equatorial region. We are therefore dealing with local source processes.

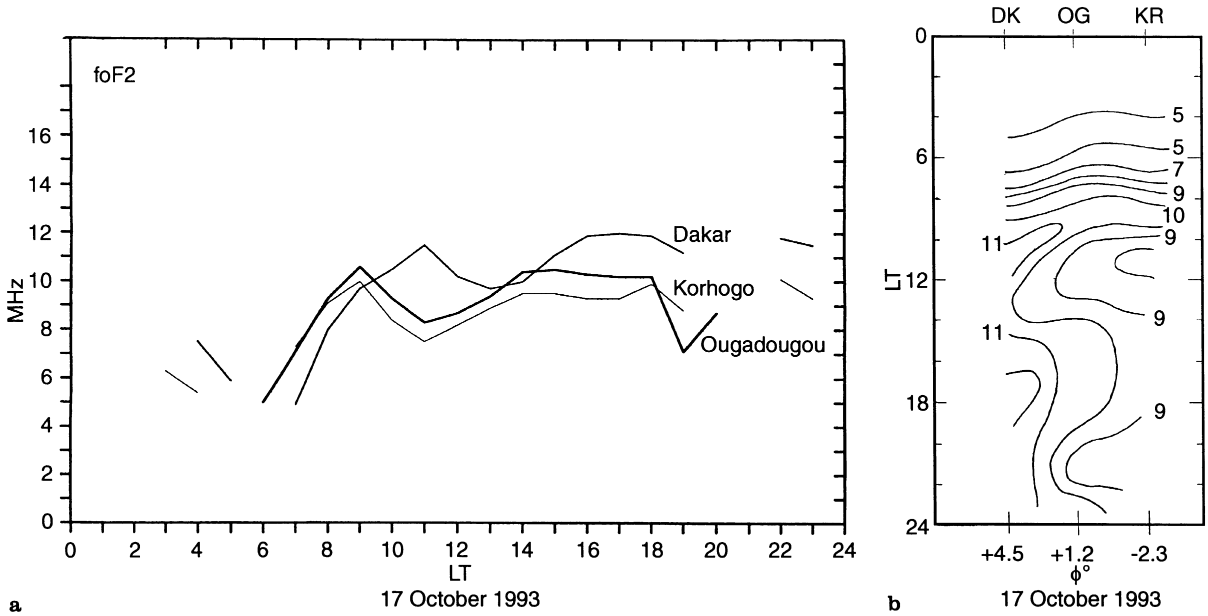

Fig. 6. Example of dome-type event, 17 October 1993. **a** *f*oF2(UT) curves, **b** corresponding *f*oF2 contour chart

3 Discussion

In situ satellite coverage of the F2 layer parameters only provide LT constructs of diurnal variations pieced together over long series of days. Such samples provide useful global averages where composite solar time changes are mixed with the poorly known "longitude effects", and with the noisy sum of UT responses from magnetospheric moment transfers: Conversely it is at low latitudes that the magnetic shell dependence of wind dynamics is maximum. The global intertropical F2 layer plasma contents are almost permanently distorted by wind drag effects according to simple seasonal cum longitude topology. For instance the HIRONO survey of average diurnal electron density at 600 km (Su *et al.*, 1996) confirms that:

1. Meridional wind-flow asymmetries in Africa are almost always the reverse of those in America, as expected from the geographic offsets of their dip equator latitudes and from the migration of the subsolar pressure bulge source;
2. Longitude sectors with divergent magnetic declination angles D show a permanent cosD reduction of the field-aligned plasma velocity.

Here we concentrate on local anomalous F2 peak distortions; we have therefore to start from strict day-to-day fluctuations. We assume longitudinal effects to be negligible as our short African magnetic tubes are little affected by declination divergence.

In standard day-time fountain (zero-order) models the magnetic field-aligned segment of near-equatorial F2 peak plasma are connected in two ways to the E layer:

a. Via the vertical $\mathbf{E} \times \mathbf{B}$ drift to the E layer electrojet source when this drift is upward, and to the upper plasmasphere reservoir when the drift is descending.

b. Via low apex height diffusion along equatorial thermosphere shells which remain isolated from the tropical plasma and connect at both ends with north and south E layer zones. Obvious first-order constraints on this model apply for the (a) connection at the centre-equatorial lower boundary of E-F1 layer transmission from the electrojet generator, and for the (b) boundaries at the upper shell surface by interactions with the meridional and zonal neutral flows.

The seasonal trends in trough and crest type abundance suggest dynamical dependence: they might be related to the large day-to-day variability of the zonal electric field even on quiet days. Lunar and solar tidal effects could be the main sources of such fluctuations (counter-electrojet events would need to be compared with our mid-morning and afternoon F layer signatures). Anderson and Matsushita (1974) analyzed the morning peak process in terms of a slowly varying $\mathbf{Vz}$ supply of plasma from the production layer under the F2 peak heights between 07.00 and 11.00 LT; this produces a peak in *f*oF2 at the end of the morning across the whole equatorial zone. If the upward drift increases very early, the resulting trough density has the shape of a high plateau without noon bite-out. In contrast with these stationary regimes our crest features have ten times faster density increases with discontinuous contours from 09.00 at the dip equator to 12.00 LT at 5° magnetic latitude (see example Figs. 4b and 6b).

3.1 Discrete character of the crest events

Usual descriptions are based on hourly *f*oF2 monthly median values which tend to smooth off most of the crest and dome equatorial variations. Nevertheless the standard model shows a general equatorial morning maximum, but this peak lasts for over 3 h, and should be almost simultaneous at the three stations. Instead we observe short LT increases and the crests evolve in the LT-latitude domain within a trough-like background; we remark that in contrast with the poor hourly resolution of the *f*oF2 plots in Figs. 1a, 4a and 6a, the continuous (LT, latitude) contours of Figs. 1b, 4b and 6b are confirmed by the quarterhourly record values; here the precise consistence of the variation allows to claim a resolution rather finer than 15 min intervals.

3.2 Dome formation

These features are remarkably simultaneous and their onsets abrupt. They require a sharper velocity gradient localized at peak F2 level, and a sufficient symmetry of the source processes, relative to the magnetic equator, to populate entirely a given magnetic tube. The similar LT distribution with crest events suggests that nevertheless the **Vz** time variation is the main cause for both types.

3.3 Qualitative model

The time-description (Sect. 2.4) suggests that crests and domes result from discrete transients. Their characteristics seem to require particular electric field sources. A sharp relative decrease in $\mathbf{E} \times \mathbf{B}$ drift would be sufficient, provided its effect is mapped to the peak F2 equatorial levels. Inside a background fountain flow of stationary vertical drift velocity as modeled by Hanson and Moffett (1966), let us create a local decrease in **Vz**: this will accumulate plasma inside a magnetic shell of about one plasma scale height thickness (see Mikhailov *et al.*, 1994). Further upwards across plasmaspheric levels, this convergence will be attenuated with distance along the drift and diffusion paths. But at *f*oF2 level it will increase the density in proportion to the local plasma reservoir (probably without modifying the total electron content). We have unfortunately no direct data on simultaneous velocity distributions (drifts, neutral winds, tide) on which to base a quantitative discussion. Since the transit time between the dynamo generator at about 130 km and the layer peak are quite short, we neglect here the delay in the rising fountain flow.

3.4 Troughs and crests relative to bulge migration

In a rough approximation both "a" trough and "c" crest-type percentages remain alike during at least ten months of the year (February to November). Starting from weak percentages between November and February the "a" and "c" types crowd into our equatorial zone from early March until September. Then trough occurrence falls off (while morning crests continue to abound until December) (Fig. 7a). Therefore the proximity of the subsolar point to our zone (11 ± 5°N geographic latitude) augments the number of nearly symmetric fountain trough cases. The early May and August intervals in 1993 are exceptions with a dip in crest abundance probably due to uniform subsolar heating across the equatorial zone. In 1994 (Fig. 7b) the seasonal trend is similar except for the August afternoon crest abundance. Thus high local heating is likely to reduce the local plasma gradients of crest (or dome) structures. The high equatorial crest and trough abundance over the ten months of bulge proximity with our domain seems to correspond to meridian wind gradients weak enough to preserve symmetrical fountain motion. But the plasma flow balance is not regularly stable with season: for instance the abrupt transition from dominant meridional wind gradient to equatorial local distortions arises just when the bulge is entering the 5°N geographic boundary of our domain between May 10 and 20.

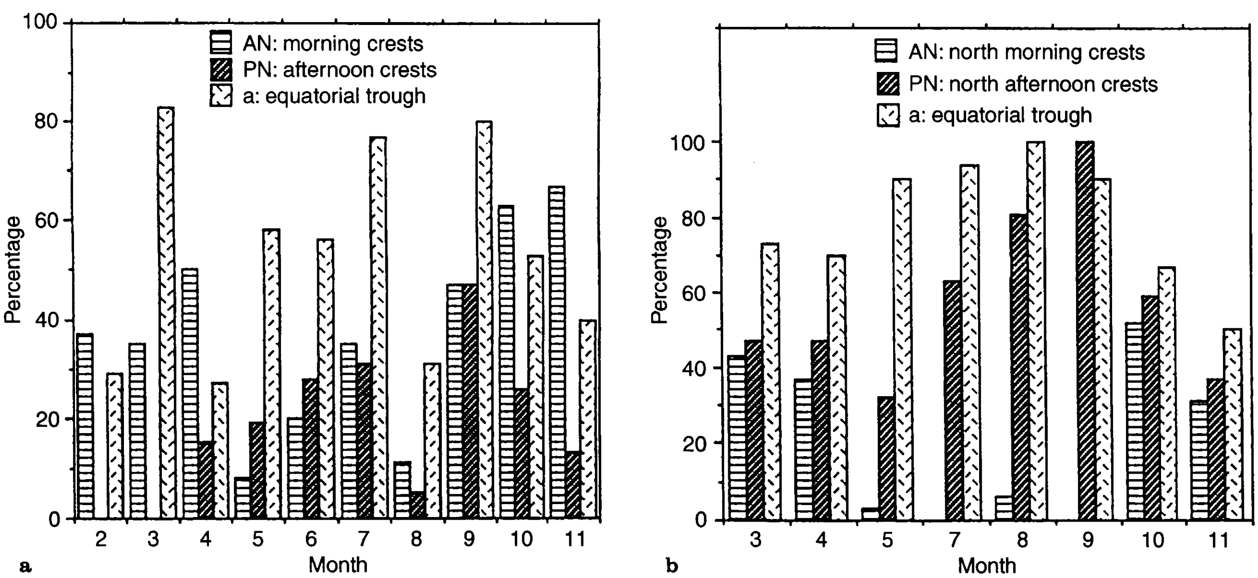

Fig. 7. **a** Monthly abundance percentages of crest and trough types in 1993, **b** same percentages for 1994

To interpret the trough occurrence we suggest that the trough shape in our *f*oF2 latitude profiles remains the background distribution imposed by the average fountain flow. Three kinds of effects contribute to fill them up in different ways:

1. Weaker *f*oF2 values, caused by faster fountain removal. This results in plateau-like profiles with shallower trough shapes (giant troughs) particularly marked when the subsolar point crosses the magnetic equator *i.e.* in April-May and August,
2. Near-equinox periods conditions where crest and domes events crowd at morning and afternoon times, filling-in the deep trough structure,
3. Boreal winter solstice, when the neutral wind gradient is producing a dominant south-to-north *f*oF2 structure.

We need to reconcile the discrete scales of our equatorial *f*oF2 crest onsets of non-systematic ("unstable") occurrence with their regular latitude progression following the large-scale fountain plasma flow.

There remains the idea that our events are triggered by large-scale gravity waves; for instance a diurnal modulation in thermospheric zonal jet intensity might theoretically create either vertically converging or diverging plasma motions of the kind required. We have looked for their possible presence on the quarter-hourly ionogram records of our three stations. Previous surveys had indeed shown such low-latitude signatures by descending strata-like distortions of a few tens of kilometers in vertical scale. But in 1993–94 in West Africa they were very rare, despite the quality of our 60-s frequency sweep ionograms.

A clue appears in the fine resolution dynamic flows generated by the latest semi-empirical Sheffield University plasmasphere ionosphere model (SUPIM) (Balan and Bailey, 1995). The model plasma flows for 1100 LT during Brazilian summer are shown in Fig. 8a. In SUPIM, coupled time-dependent equations of ion mass continuity, momentum and energy balance are solved along closed magnetic field lines between base altitudes of about 130 km in conjugate hemispheres. The outputs are the densities, plasma fluxes and temperatures of the electrons, and of the O^+, H^+, N_2^+, O_2^+ and NO^+ ions. The geomagnetic field is represented by an eccentric dipole and the neutral temperatures are determined from MSIS-86 (Hedin, 1987), the neutral wind from HWM90 (Hedin *et al.*, 1991). The vertical $\mathbf{E} \times \mathbf{B}$ drift velocity model used in the present simulation is constructed from measurements made at Jicamarca and from results of previous studies as described in Jenkins *et al.* (1997). Temporal plots of the vertical $\mathbf{E} \times \mathbf{B}$ drift used in the model calculations are shown in Fig. 8b, the drifts are shown for southern summer, winter and equinox (for low solar activity).

The latest example (Fig. 8a) corresponds to solar flux decline and conditions similar to the May–August 1993 period for West Africa. It is relevant to our assumption of flow convergence. It shows an area of F2 peak non-divergent angular **NV** flow vectors located about the −8° dip latitude by 450 km altitude segment. On such a local background an additional convergent **Vz** slowdown is easily maintained whereas the adjacent segments (from −5°, 500 km to +4°, 400 km) evolve with angularwise divergent flows that would erase our assumed **Vz** convergence.

The conditions for morning crest formation would therefore be two in particular the general upward **Vz** relative decrease and a further abrupt downward perturbation while the **Vz**-controlled flows still persists.

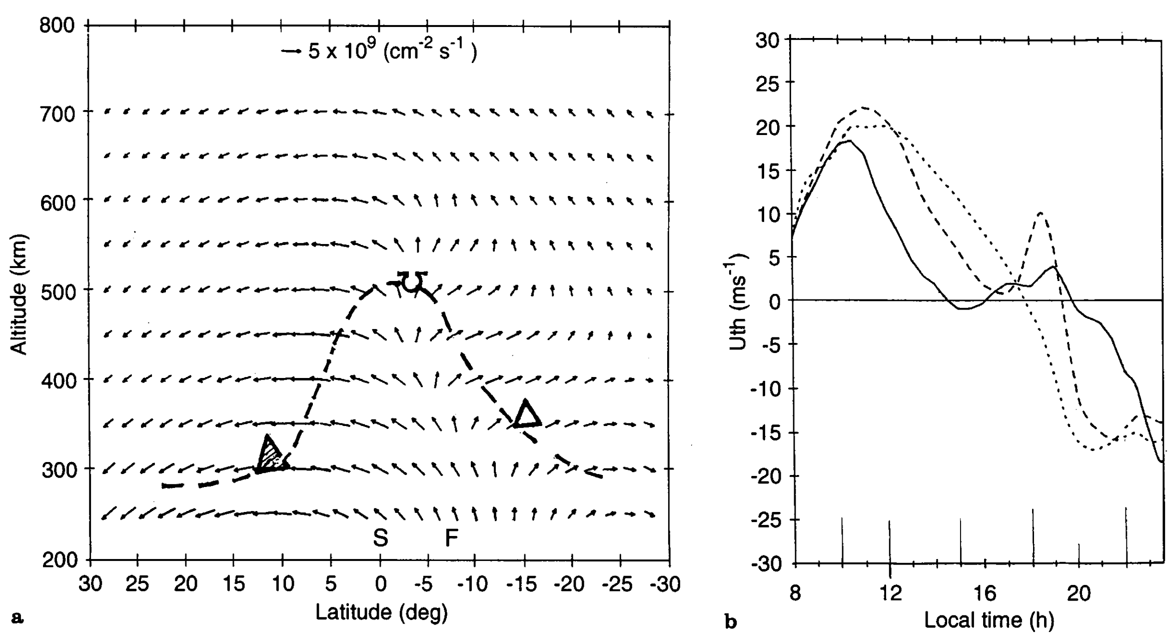

Fig. 8. **a** Meridian section with NV flow vectors, SUPIM model for Brazil Summer 1100 LT, solar flux F10.7 = 85. Ʊ: trough; Δ: tropical crest; - - - -: hMF2 line. **b** Jicamarca Vz(LT) curves for three seasons (Solar flux minimum). The *curve* used for the present SUPIM simulation is the Summer case (solid line).

3.5 Dome fluctuations

The month of March 1993 becomes a stormy period after March 5. It then shows many more crests and less domes (Figs. 7a and 9a). For the rest of the year domes exhibit no simple dependence on seasonal phase. Afternoon domes appear mostly around transition periods like winter "equinox" (April) and "autumn" (August). Morning domes have a similar annual phase, but while they remain visible during the December solstice, they show seasonal peaks in February and October, and disappear from June to August. These changes might be due to a seasonal variation in the **Vz** diurnal changes (Fig. 8b). Apart from possible magnetic auroral wind disturbances we need local types of coupling to explain these "d" types. In 1994 domes are much less frequent, and the summer minimum of occurrence lasts until September (Fig. 9b).

Lack of space and time resolution prevented the previous workers identifying the quiet-day equatorial domes among the pre- and post-noon larger maxima. Since the moment transfers from auroral sources were then unsufficiently understood, it was difficult to time the disturbance dynamo processes and associated thermospheric fronts. Our results will provide significant material for distinguishing such perturbations from the local thermospheric sources proposed here.

3.6 Magnetic field-orthogonal "e" gradient types

These contours and statistics are not illustrated here. These distortions dominate our *f*oF2 contours throughout both years' November to February solstices between 10:00 and 20:00 UT. The obvious explanation for such strong and stable south-to-north *f*oF2 gradients is a local equalization of opposite fountain and subsolar bulge flow (convergence) around geographic latitudes of 08° to 12°N, locally slowing down the southward fountain flow.

The consistency of our interpretation could be disputed as we are piecing together the SUPIM quasi-stationary simulation of vertical drift and meridian wind flows with a transient drift-only perturbation.

3.7 A possible alternative

Another scheme might explain the abrupt morning domes by delayed occurrence of the classical pre-noon peak (or plateau) shape of the *f*oF2(LT) variation. It assumes after 08.00 LT a rapidly increasing drift velocity (with **Vz** about 100 m s^{-1}) across the whole domain up to $h_A = 700$ km, together with low F2 peak initial densities in the $225 < h_A < 325$ km magnetic shell; a relative depletion can be maintained until 09.30 LT if non-local sunrise photo-electron heating persists within the whole peak segment of this shell. Photo-electrons are mostly produced at 160 to 220 km levels at the north and south ends of the shell, i.e. in two segments located between 05° and 08° dip latitude. After 08.30 the plasma density increase caused by growing ionization must preferentially replenish the F1 and bottom F2 levels. When the magnetic tube content reaches a critical threshold that interrupts heating at the dip equator, the normal morning peak profile is suddenly rebuilt across the F2 peak shell and the dome appears. Here again the dip winter solstice November to February conditions of unimpeded neutral flow in Africa appear sufficient to prohibit trough and dome structures.

This scheme makes fewer assumptions than the **Vz**(t) profile mechanism suggested in Sect. 3.4 and 3.5, but it needs validation by detailed time-simulation of the coupled fountain and heating contributions in the meridian domain of small equatorial magnetic tubes.

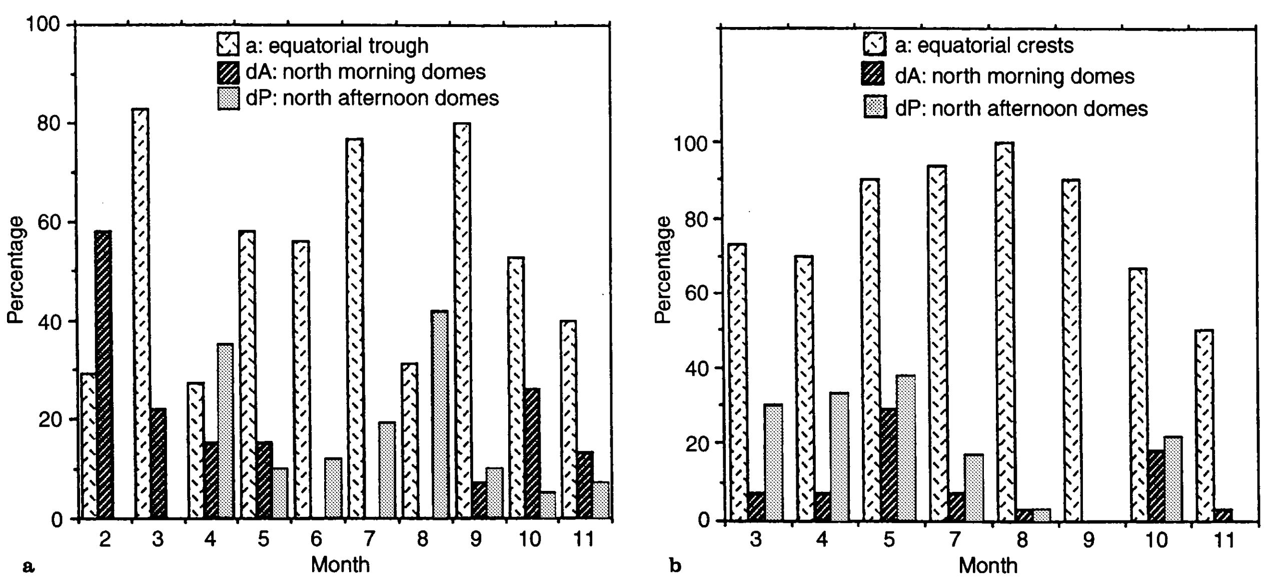

Fig. 9. a Monthly abundance percentages of dome and trough types 1993, **b** same percentages for 1994

At the present time these qualitative suggestions seem to us the only possible approach to the recurrent non-stationary crest and dome processes. The afternoon crest events remain sometimes poorly separable from the main subtropical crests returning towards the dip equator (this uncertainty should be lifted when the LETTI "STUDIO" HF radar is able to track the entire intertropical zone from Korhogo).

4 Summary

Our results establish the frequent existence of a double system of ionization crests in the low-latitude F2 layer distribution.

The inner magnetic shells of apex heights 200 km $< h_A <$ 450 km are frequently shaped in thin, evolutive, latitude-LT crests that striate the equatorial background trough distribution. Less frequently the entire zone is barred by a rapidly rising field-aligned dome. Both types have clear LT occurrence control. They start around the dip equator at mid-morning and early afternoon hours. Their onsets coincide with transitional periods in the diurnal electric field variation which controls the vertical plasma flow at F2 peak levels.

Except for some of the most severe magnetic storms when the trough zone is invaded by large F2 ionization domes, our equatorial crests and domes show no clear dependence on planetary magnetic field activity.

The former problem of equatorial "noon bite-out" fluctuations is gaining fuller interpretation. Comparison of past and present African results allows us to claim important solar activity changes in the diurnal *f*oF2 regimes between the low 1966 and the declining 1993 solar flux periods.

For the IEEY period final interpretation, we hope soon to compare our results with relevant Indian and Brazilian series that should provide experimental comparisons and independent diagnostics of our dynamical schemes.

We leave for further publication the detailed study of the couplings between **Vz** direct drift and other dynamic moments. These must include: (1) zonal wind profile changes, and (2) parallel forcings exerted by normal ion fountain diffusion, neutral pressure thermospheric bulge boundaries and photo-electron heating gradients.

Two problems of electrodynamic transients deserve fine structure modelling in the ($2\frac{1}{2}$ D, t) space around the dip equator. We need detailed solutions of the current continuity equations and generalized Ohm's law throughout longitude-local time coverages from 06.00 to 18.00 LT: firstly, to identify the mixed dependence of **E**-field dominated versus **J**-connected equatorial dynamo areas and phases during conditions respectively of normal electrojet formation, diurnal reversal phases, and the two kinds of "counter-electrojet" events; secondly, to deduce magnetic shell mapping into F layer tube segments connecting with the E layer boundary between the central vein of the electrojet and its lateral wings; and thirdly, to take into account the special fountain discontinuity between meridian field-aligned flows and magnetic field-perpendicular drift motions.

The coming solar minimum period should see developments of HF radar tracking of the E and F layer structures. These will allow latitude extensions of our network, and progress towards climatology of travelling $\mathbf{U}_d$ events as well as the variety of crests and domes.

These structures are not merely exciting objects of research, but as gradient bearers they will allow efficient HF telecommunications via the equatorial ionosphere.

Acknowledgements. The French participation in IEEY is due to the international IAGA inspiration by Keith Cole and Roger Gendrin. The revival of the Korhogo site and the maintenance of the three ionosondes have been managed by the French CNET Lannion/B, thanks to Jacques Papet-Lépine, with ionospheric stations equipped and their personnel trained under Dr Rudi Hanbaba and M. Jean Henry. Our thanks go to the magneticians who followed Pierre-Noël Mayaud at IPGP, and to Dr Jacques Vassal then at ORSTOM Dakar. The Franco-African teams have set an example of developing instruments, mutual training and research methods especially at both Universities of Abidjan and Dakar. We are indebted to Barbara Jenkins for providing the SUPIM results and for decisive discussions. Two referees gave worthwhile evaluation and comments on our work.

Topical Editor D. Alcaydé thanks two referees for their help in evaluating this paper

References

Abur-Robb, M. F. K., and D. W. Windle, On the day and night reversal in NmF2 north-south asymmetry, *Planet. Space Sci.*, **17,** 97, 1969.

Anderson, D. N., A theoretical study of the ionospheric F region equatorial anomaly. I., theory, *Planet. Space. Sci.*, **21,** 409–419, 1973.

Anderson, D. N., Modeling the ambient, low latitude F region ionosphere a review, *J. Atmos. Terr. Phys.*, **43,** 753–762, 1981.

Anderson, D. N., and S. Matsushita, Seasonal differences in the low latitude F_2 region ionization density caused by $\mathbf{E} \times \mathbf{B}$ drift and neutral wind, *J. Atmos. Terr. Phys.*, **36,** 2001–2011, 1974.

Appleton, E. V., Two anomalies in the ionosphere, *Nature*, **157,** 691, 1946.

Appleton, E. V., Equatorial Anomaly in the F2 layer of the ionosphere, *Some ionospheric results obtained during the IGY*, Elsevier Publications, Amsterdam, 1960.

Balan N., and G. J. Bailey, Equatorial plasma fountain and its effects: Possibility of an additional layer, *J. Geophys. Res.*, **21,** 421–21, 432, 1995.

Coley, W. R. and R. A. Heelis, Low latitude zonal and vertical ion drifts seen by DE2, *J. Geophys. Res.*, **94,** 6751–6761, 1989.

Duncan, R. A., The equatorial F region of the ionosphere, *J. Atmos. Terr. Phys.*, **18,** 89–100, 1960.

Fejer, B. G., and E. R. de Paula, Global equatorial ionospheric vertical plasma drifts measured by the AE-E satellite, *J. Geophys. Res.*, **100,** 5769–5776, 1995.

Hanson, W. B., and R. J. Moffett, Ionization transport effets in the equatorial F region, *J. Geophys. Res.*, **71,** 5559–5572, 1966.

Hedin, A. E. *et al.*, MSIS-86 thermospheric model, *J. Geophys. Res.* **7,** 657, 1991.

Hedin, A. E. *et al.*, Revised global model of thermospheric winds using satellite and ground-based observations, *J. Geophys. Res.*, **96,** 7657–7688, 1991.

Jenkins, B., G. J. Bailey, M. A. Abdu, I. S. Batista and N. Balan, The formation of an additional layer in the equatorial topside ionosphere, *Annales geophysicae* (1997 in press).

Lyon, A. J., and L. Thomas, The F2 region equatorial anomaly in the African, American, and East Asian Sectors during sunspot maximum, *J. Atmos. Terr. Phys.*, **25**(7)**,** 373–386, 1963.

Martyn, D. F., Atmosphere tides in the ionosphere.1. Solar tides in the F2 region, *Proc. R. Soc., London*, **A89,** 241, 1947.

Milkhallov, A. V., M. Förster, and M. G. Skoblin, Neutral gas composition changes and $\mathbf{E} \times \mathbf{B}$ vertical plasma drift contribution to the day equatorial F2-region storm effects, *Annales Geophysicae*, **12,** 226–231, 1994.

Rastogi, R. G., Magnetic control on the variations of the critical frequency of the ionosphere, *Can. J. Phys.*, **37,** 874, 1959.

Su Y. Z., K. Y. Oyama, G. J. Bailey, S. Fukao, T. Takahashi, and H. Oya, Longitudinal variations of the topside ionosphere at low latitudes: Satellite measurements and mathematical modelings, *J. Geophys Res.*, **17,** 191–17, 205, 1996.

Vila, P. M., Intertropical F2 ionization during June and July 1966, *Radio Sci.* **6, 7,** 689–697, 1971.

Vila, P. M., New dynamic aspects of intertropical F2 ionization, *Radio Sci.*, **6, 11,** 945–954, 1971.

Walker, G. O, Longitudinal structure of the F region equatorial anomaly. A review, *J. Atmos. Terr. Phys.*, **43,** 763, 1981.